Earthquake Geotechnical Engineering for Protection and Development of Environment and Constructions – Silvestri & Moraci (Eds)
© 2019 Associazione Geotecnica Italiana, Rome, Italy, ISBN 978-0-367-14328-2

Shallow foundation liquefaction-induced settlements of residential buildings due to man-induced earthquakes

Y. Chaloulos, A. Giannakou, V. Drosos, P. Tasiopoulou & J. Chacko
GR8 GEO, Athens, Greece (formerly Fugro)

S. De Wit
Shell Global Solutions International B.V.

ABSTRACT: This paper focuses on the evaluation of the dynamic performance of existing residential houses affected by the occurrence of gas-extraction-induced earthquakes. Nonlinear, effective stress, fully coupled, dynamic soil-structure interaction analyses were performed to develop estimates of liquefaction-induced settlements for buildings on narrow spread footings. The analyses covered the range of soil conditions, ground motions and structural characteristics that are typically encountered in the study area. Results verify patterns observed in recent studies for slab foundations and shed light on new mechanisms. For the low magnitude earthquakes considered in this study the total foundation settlements were found to be relatively limited. A simplified equation was developed from regression of the numerical analyses results to derive estimates of liquefaction-induced settlements for residential buildings that was adopted in the latest update of the relevant building code for the area.

1 INTRODUCTION

An extensive numerical study was undertaken to investigate liquefaction-induced settlements of existing residential buildings on spread footings subjected to gas-extraction-induced earthquakes. The project area is in northern Europe where tectonic seismicity is very low, thus most structures have not been designed to resist earthquake loading.

Recent studies on liquefaction-induced settlements of shallow foundation (for example Dashti and Bray 2013; Karamitros et al. 2013; Karimi et al. 2018; Macedo and Bray 2018) focus on buildings resting on continuous rigid slab foundations (i.e. minimum footing widths of about 6 meters) subjected to relatively large earthquake events (i.e. corresponding to magnitudes larger than $M_w = 6$), typically associated with a significant number of loading cycles. As a result, their findings could not be readily applied to the buildings of the present study, which involves (a) spread footings of small width which might experience different deformation patterns than the wide rigid slabs previously studied, and (b) earthquakes of medium intensity ($M_w \approx 5.0$) typically associated with small number of loading cycles. Furthermore, under these conditions, the contribution of post-seismic volumetric settlements as a fraction of the total settlements might be more important, thus a more detailed approach to estimate the magnitude of post-seismic volumetric settlements was also required.

Nonlinear, effective stress, fully coupled, dynamic soil-structure interaction analyses were performed to evaluate liquefaction-induced settlement of narrow spread footings supporting existing residential buildings under moderate shaking levels. The results of the detailed analyses were then used to develop a simplified equation for the estimation of settlements. Calibrated advanced constitutive models were used to simulate the complex behaviour of loose sands with emphasis also given to the estimation of post-seismic deformations. Validation of the adopted numerical approach against a case history is also presented.

2 MODELING APPROACH

2.1 *Overview*

Two-dimensional, dynamic, effective stress analyses were performed with the finite difference code FLAC v8.0 (Itasca 2016). The seismic performance of the foundation was evaluated for two stages: a) during seismic shaking (i.e. co-seismic); and b) after the end of seismic shaking (i.e. post-seismic). The first stage analyses (co-seismic) involves performing dynamic, nonlinear, effective stress analyses with the PM4Sand constitutive model (Boulanger and Ziotopoulou 2017) for sands to identify zones that liquefy and the deformations that occur during strong shaking (primarily shear-induced settlements). Two independent types of analyses were performed for the second stage (post-seismic), both of which are static analyses under gravity loads with the following objectives: i) estimate the post liquefaction volumetric-strain induced settlements (i.e. settlement analyses) and ii) assess the foundation stability assuming residual undrained shear strength conditions in the liquefied zones under the foundation (i.e. stability analyses).

Post-earthquake reconsolidation settlements occur as excess pore water pressures dissipate and the soil's effective stress increases. This type of settlements is typically estimated from empirical free-field reconsolidation methods (e.g., Ishihara and Yoshimine 1992) since they are difficult to model numerically. This is because a large portion of the post-earthquake reconsolidation strains occur with a constant stress ratio. This cannot be directly captured by stress-ratio driven models like PM4Sand, typically used in liquefaction analyses, where plastic strains occur with change in stress ratio. However, PM4Sand employs an empirical scheme outside of the plasticity formulation (empirically reducing the elastic shear modulus) to calculate post-shaking reconsolidation strains. A comparison between the post-earthquake reconsolidation settlements estimated using PM4Sand's scheme and the procedure described below based on the Ishihara and Yoshimine (1992) empirical correlation between shear and volumetric strains, indicated that the latter predicts somewhat larger reconsolidation settlements for the range of conditions relevant to this study. Thus it was decided to conservatively adopt the procedure described below. The post-seismic stage of estimation of post-earthquake reconsolidation settlements followed the co-seismic stage and involved a static analysis under gravity loads with a Mohr-Coulomb constitutive model and updated stiffness parameters for zones where the maximum excess pore pressure during shaking (i.e. co-seismic stage) exceeded a specified threshold (typically 70 percent), indicative of significant pore pressure generation. The updated stiffness parameters of the selected zones were estimated through the constrained modulus using:a) the empirical relationship by Ishihara and Yoshimine (1992) between maximum shear strains that developed during the earthquake (co-seismic stage) and volumetric strain and b) a Poisson's ratio of 0.3. The above procedure for the volumetric settlement estimation was applied in the modeling of the Port Island Case Study (Ishihara et al. 1996; Ziotopoulou and Boulanger 2013) and predicted reconsolidation settlements on the order of 30 cm which are within the reported 20 to 50 cm range.

Post-earthquake stability may be critical even if stability is ensured during shaking as has been demonstrated in documented case histories (e.g. lower San Fernando dam case history). Void redistribution and soil mixing can give post-liquefaction strengths much lower than those from undrained laboratory tests. Although fully coupled effective stress numerical analyses such as those performed for the co-seismic stage can give important insight into the process, further development and calibration is needed (Naesgaard & Byrne, 2007). In the meantime, a procedure combining effective-stress analysis during strong shaking and total-stress analysis at the post-earthquake stage proposed by Naesgaard & Byrne (2007), which has successfully captured soil liquefaction during strong shaking and the triggering of catastrophic slope failure after strong shaking, was used for to check the post-earthquake stability of the foundation. The post-seismic stage followed the co-seismic stage and involved static stability analyses under gravity loads and residual conditions obtained at the end of shaking, such as stiffness and strength degradation due to liquefaction. The post-seismic analyses included the following steps: (1) specifying a typical threshold indicative of liquefaction occurrence or severe soil softening, such as excess pore water pressure ratio, r_u, being greater than 0.7, (2) identifying the elements where the threshold (r_u > 0.7) was exceeded at any point during shaking (co-seismic stage), (3) updating the constitutive

model applied to the these elements to Mohr–Coulomb and assigning a residual strength based on empirical relationships by Idriss and Boulanger (2008) assuming void redistribution effects, and (4) conducting static analyses under gravity loads until equilibrium is reached.

2.2 *Soil constitutive models and model calibration*

The response of liquefiable sands was simulated with the PM4Sand constitutive model (Boulanger and Ziotopoulou 2017). The model was calibrated to capture liquefaction triggering and shear strain accumulation behavior for both level (no-bias) and sloping ground (bias) conditions following methodologies described by Giannakou et al. (2011) and Tasiopoulou et al (2018). Particularry, calibration against liquefaction triggering at low number of cycles corresponding to $M_w \approx 5$ earthquakes was based on empirical liquefaction resistance curves by Green et al (2018) for level ground conditions (no-bias). For sloping ground conditions (static bias) the recommendations of Idriss and Boulanger (2008) were adopted.

2.3 *Modeling of structures and foundations*

The structural members were simulated with linear elastic beam elements described in terms of mass density, ρ; Young's modulus, E; cross-section area, A, and moment of inertia, I. The footings were simulated as elastic solid elements. Interface elements were placed at the base and at the vertical side of each footing following an elastic-perfectly plastic law and a friction angle of 35 degrees.

3 VALIDATION OF NUMERICAL APPROACH: CASE HISTORY OF RESIDENTIAL BUILDING AT KAIAPOI, NEW ZEALAND

The numerical approach described above was validated against a case history, modeling conditions as similar as possible to the ones at hand. A residential building with largely similar structural and foundation characteristics to the residential buildings considered in this study and subjected to liquefaction-induced settlements during the 2010–2011 Canterbury, New Zealand earthquake sequence was selected as validation case. Information about the building characteristics, observed settlements and geotechnical conditions were gathered by BICL (2018).

The 2010–2011 Canterbury earthquake sequence includes the 4 September 2010 M_w=7.1 Darfield earthquake and the 22 February 2011 M_w= 6.2 Christchurch earthquake among other events. The residential building analyzed is a two-storey unreinforced masonry and timber framed construction founded on strip footings along the perimeter of the building. It is located at Kaiapoi, approximately 16 km north of the Christchurch Central Business District. According to information gathered by BICL the building suffered differential settlement during the M_w= 7.1 Darfield earthquake event (September 2010) with the Eastern side of the building reported to have settled about 5–10 cm. Little additional settlement was reported for the subsequent M_w=6.2 Christchurch earthquake event (February 2011).

Idealized stratigraphy and properties were developed based on the CPT data at the north and eastern corners of the building for depths 10m and 7m below the ground surface, respectively. For greater depths up to 18m (i.e. top of Riccarton gravel and the base of the numerical model, Figure 1), the soil profile of the Kaiapoi North School (KPOC) station (Wotherspoon et al 2013), situated about 700 m north of the building, was used. The values of relative density D_r for the soil profiles at each corner were based on the Boulanger and Idriss (2014) correlation with CPT data.

Figure 1 presents the model mesh together with the idealized stratigraphy and relative density values assigned to the sand layers. The equivalent frame is also shown on Figure 1 and has a fundamental period of 0.08 sec. The static load exerted on the soil is estimated to be 45 kN/m approximately with a foundation width of 0.8 m. The liquefaction triggering curve for the critical surficial layer with the lowest relative density of 40–45% was obtained from the laboratory testing results of Christchurch fluvial silty sand by Taylor et al. (2013), shown on Figure 1. The calibration of PM4Sand (Figure 1) was based on the lab data for this layer, and judgment was used to scale up the resistance to liquefaction triggering of the layers with higher relative density.

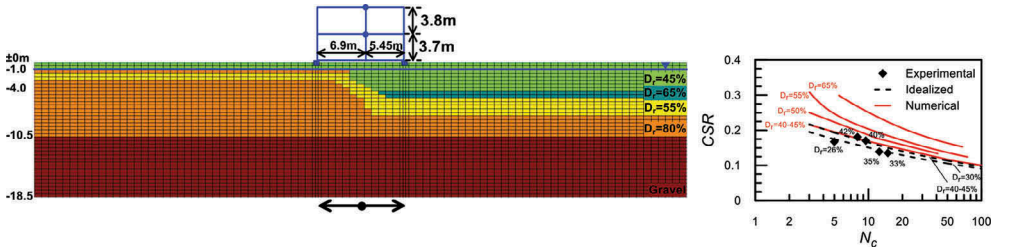

Figure 1. Numerical model used for Kaiapoi case history, input acceleration time histories and liquefaction triggering curves for various relative densities.

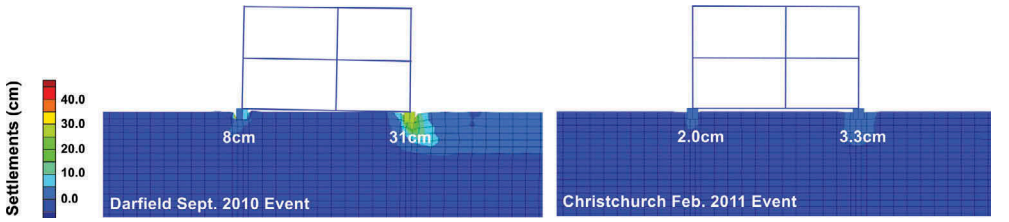

Figure 2. Settlement contours at the end of shaking for Darfield (left) and Christchurch (right) event.

Markham et al. (2014) suggest that the Riccarton Gravel formation, which is encountered at depths less than 40m from the ground surface in the wider area surrounding Christchurch, can be considered stiff enough to be selected as engineering bedrock. The deconvolved Riccarton gravel level ground motions (fault-normal and fault parallel components) obtained from the CACS recording by Markham et al. (2014) were used as input motions for the numerical analyses applied at 18 m depth. However, it was observed that the Markham et al. (2014) proposed scaling factor of 0.47 for the Darfield event, resulted in large residual values at the KOPC location. To improve the prediction for the Darfield event at KOPC, a higher scaling factor equal to 1.0 was used for the Darfield event resulting from 1D site response analyses using the KPOC soil profile (Wotherspoon et al 2013). The deconvolved Riccarton gravel level ground motions were rotated to the building coordinates and the component parallel to the northeastern section was selected (Figure. 1).

Figure 2 presents numerical results in the form of settlement contours for the Darfield and Christchurch events. For the Darfield event, the settlement contours show that the right (eastern) footing settles 26 cm and the left (northern) one settles only 8 cm resulting in a differential settlement of about 18 cm. For the subsequent Christchurch event significantly lower differential settlements in the order of 1.3 cm are estimated which is in line with observations of little additional differential settlement for the building after this event. The comparison of field observation during the different earthquake events with numerical model predictions is considered satisfactory considering the uncertainties and subsequent simplifications involved.

4 INPUT PARAMETERS FOR THE NUMERICAL MODELS

Parametric 2D dynamic soil structure interaction analyses were performed for typical residential buildings in the study area by varying key parameters that affect the system behavior such as non-liquefiable crust thickness, H_{cr}, liquefiable layer thickness, H_{liq}, liquefiable layer relative density, D_r, undrained shear strength of liquefiable crust, $S_{u,crust}$, foundation pressure, Q, foundation width, B, building typology, and ground motion characteristics.

In total, more than 500 analyses were performed for the parameter values presented in Table 1. The typical geometry of the numerical model used in the parametric study is shown

Table 1. Range of values considered in the parametric study.

Parameter	Description	Range
H_{liq} (m)	Liquefiable layer thickness	0.5 - 10.0
D_r (%)	Liquefiable layer relative density	30 - 50
H_{cr} (m)	Non-liquefiable crust thickness	0.5 - 1.0
$\alpha = (\pi+2)\ S_{u,crust}/q$	Undrained shear strength of crust as a function of the foundation pressure, q	1.0 - 10.0
B (m)	Foundation width	0.25 - 0.70
Embedment Depth (m)	Foundation Embedment Depth	0.45 - 0.90
Q (kPa)	Foundation pressure	20 - 120
$PGA_{,surf}/Sa_{0.7\ sec,\ surf}$ (g)	Ground Motion Spectral Accelerations	0.10 – 0.30/0.27 – 0.55
D_{5-75} (s)	Ground Motion Significant Duration	2.6 - 10.4
LPI_{ISH}	Liquefaction Potential Index	<1 - 22
T_{st} (s)	Fundamental Structural Period	0.11 – 0.22
Number of Storeys	Structure	1 – 2

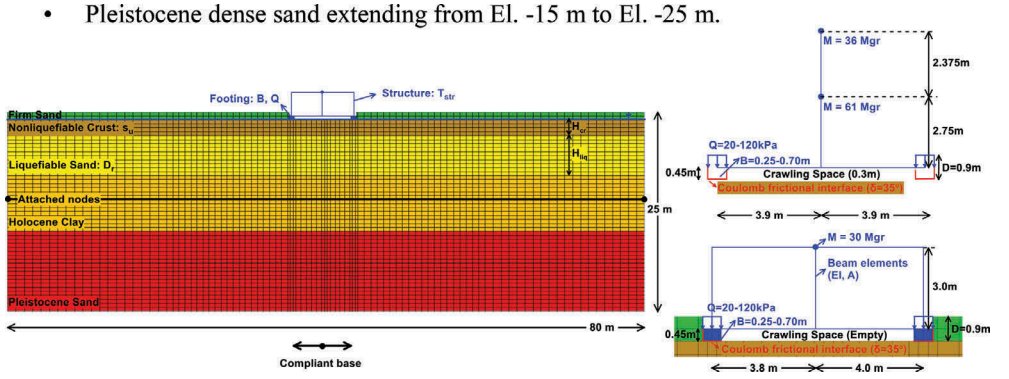

Figure 3. Numerical Model Geometry.

on Figure 3. The following idealized stratigraphic ranges were developed based on data from 40 Cone Penetration (CPT) Tests in the study area:

- Top soil consisting of non-saturated sand extending from the ground surface at El. 0 m to foundation level (varying between El. -0.5m and El. -0.9 m).
- Non-liquefiable crust layer of varying thickness, H_{cr}.
- Liquefiable layer of varying thickness, H_{liq}.
- Holocene stiff clay layer extending to El. -15 m.
- Pleistocene dense sand extending from El. -15 m to El. -25 m.

The undrained shear strength of the Holocene stiff clay layer varied with depth from 20.0 to 40.0 kPa. A friction angle of 40 degrees was used for the Pleistocene dense sand. The hydraulic conductivity of the liquefiable sand layers was considered anisotropic and equal to 10^{-6} m/s and $5x10^{-7}$ m/s for horizontal and vertical drainage, respectively.

Two structures, representative of the residential building stock in the project area were considered in the analyses: i) a 1-storey masonry detached house with an attic and ii) a 2-storey house. The 1-storey structure is 7.8 m by 10.7 m in the transverse and longitudinal directions respectively. Its foundation system consists of strip footings, mainly along the perimeter of the building. The 3D structure was incorporated in the analysis by introducing an equivalent 2D frame model with properties provided by the structural engineers and a fixed-base period of 0.11 sec (Figure 3). The 2-storey house is 7.8 m wide and has a tributary out-of-plane length of 6.3 m and a fundamental period of 0.22 sec. A multiple degree of freedom oscillator with two concentrated masses was used

to model this structure (Figure 3). As shown on Figure 1 the crawl space between the foundations is empty for the 1-storey house and filled with 30 cm of soil for the 2-storey house.

Eleven acceleration time histories were developed and applied as outcrop motions at the base of the numerical model (El -25 m). The key characteristics of the eleven ground motions in terms of amplitude and significant duration, D_{5-75}, are summarized in Table 1.

5 PARAMETRIC NUMERICAL ANALYSES RESULTS

Representative results and trends observed from the parametric analyses are briefly discussed below. Figure 4b shows example contours of maximum excess pore pressure ratio during shaking superimposed with displacement vectors at the end of shaking (D_r=40%, H_{cr}=0.0, Q=36.0kPa, B=0.7m). Also shown (Figure 4a) from top to bottom are time histories of left and right foundation settlements (black and red line respectively), excess pore pressure ratio at the free field and below the footing (black and red line respectively) and acceleration at the base and directly below the footing (black and red line respectively). As shown on the figure the soil does not fully liquefy, a result of the medium intensity of the input motion. Large excess pore pressure ratios (r_u > 0.9) and soil liquefaction only develop in a narrow zone, approximately 0.5 to 1.0 m thick, close to the base of the layer. This reduces the magnitude of strength degradation and subsequent deformations. The small footing width results in a rather small stress bulb, which is mostly interacting with the nonliquefied soil at shallow depths and not with the deeper liquefied soil. Moreover, as the direction of the displacement vectors suggests, the weight of the soil at the outer edges of the footings, in combination with the softening of the underlying sand, creates a spiral deformation mechanism, which pushes the soil below the structure upwards, as if the embedment was a strip footing of large width. Because of the above, calculated settlements are rather small, in the order of 3.0 cm. It is also noteworthy that, as a result of relatively low excess pore pressure build-up, the motion transmitted to the foundation is not de-amplified compared to the input motion. This natural isolation mechanism has been systematically observed in other studies, which, however, concerned strong input motions and extensive soil liquefaction. Finally, as shown in the figures, differential settlements were low (less than 0.5%) in the absence of lateral stratigraphic variations.

Regarding the influence of the various parameters considered, the following main observations were made:

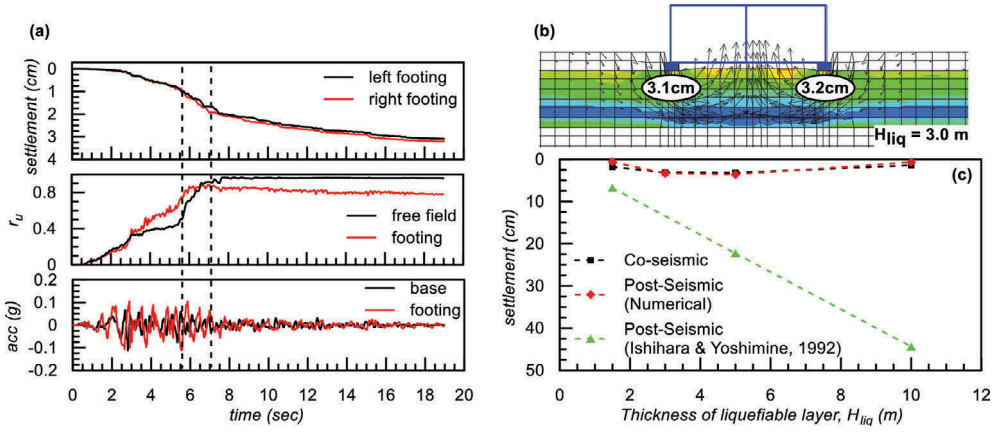

Figure 4. (a) Time histories of acceleration at the base of the model and below the footing, footing settlement and excess pore pressure ratio at the free field and below the footing (b) Maximum excess pore pressure ratio during shaking and displacement vectors at the end of shaking (c) Contribution of co-seismic, shear-induced and post-seismic, volumetric-induced settlements on the total settlements of the foundation.

- Relative density of liquefiable sand. For D_r values of 50% or more estimated settlements are practically negligible and remain below 1 cm for all cases, as a result of minor excess pore pressure build-up.
- Thickness of liquefiable sand. Estimated settlements increase with H_{liq}, however, beyond a certain point, a plateau is formed, and settlements are not affected by further increase in sand thickness. Finally, for very thick sand layers, further increase in sand thickness causes footing settlements to decrease. This type of response has been also observed in recent studies (Karimi et al. 2018) and has been attributed to the natural base isolation mechanism created by the liquefied soil layers.
- Non-liquefiable crust. The presence of crust can drastically reduce foundation settlements. The benefit of the presence of the crust is less pronounced as the strength of the crust decreases. When the crust is soft it also deforms, thus leading to the accumulation of extra foundation settlements.
- Foundation load. Increase in foundation load leads to increase in footing settlements, however with a constantly decreasing rate. This response has also been observed in other studies (Karamitros et al. 2013; Karimi et al. 2018; Macedo and Bray 2018) and is attributed to factors such as the increase in confinement and the shear-induced dilative response of the soil below the footing as settlement accumulation increases.
- Foundation width. Results suggest an approximately linear increase in settlements as the width of the footing increases. However, it should be noted that the influence appears to be relatively small, while the range of values analyzed is not very wide (B=0.25–0.7m).
- Ground Motion Characteristics. Foundation settlements increase systematically with ground motion intensity measures such as Arias Intensity, D_{5-75}, CAV, CAV_{dp}, with the latter two providing an overall better correlation. Regarding spectral content, foundation settlements do not correlate well with PGA since the high-frequency components do not affect liquefaction related phenomena, while a better correlation is observed with spectral accelerations at longer spectral periods (i.e. 0.7 sec), which are closer to the soil's and to the structure's period (taking into account Soil-Structure-Interaction).

Figure 4c presents the shear-induced and volumetric settlements versus liquefiable sand thickness (D_r=40%, Q=36kPa). The black line shows the co-seismic (primarily shear-induced) settlements and the red the corresponding reconsolidation settlements (primarily volumetric and calculated numerically with the procedure described above). A second set of volumetric settlement estimates, shown in green, was obtained using the empirical chart by Ishihara and Yoshimine (1992) after performing a liquefaction triggering analysis using the Green et al (2018) empirical correlation. As shown, the accumulation of volumetric settlements follows the same trend as the co-seismic, i.e. they initially increase with H_{liq} until they reach a plateau, while, for large thicknesses, they subsequently decrease. However, this does not necessarily imply that volumetric settlements depend on the corresponding shear-induced settlements. In general, volumetric settlements are the direct result of excess pore pressure build-up, while shear-induced settlements are the result of much more complex mechanisms. For instance, in the case of a footing resting on a thick crust underlain by a thick liquefiable layer, shear-induced settlements would be minor, however, excess pore pressure build-up within the sand would yield large volumetric settlements. It is noted that for the case shown in the figure as well as for most of the cases analyzed, the post-seismic reconsolidation settlements estimated numerically are on the same order of magnitude as the co-seismic settlements. Finally, it is noticeable that the simplified 1-D analytical procedure leads to significant overestimation of volumetric settlements. This is primarily because the analytical methodology overestimates the extent of liquefaction and thus excess pore pressure development, while, as described above (e.g. Figure 5) liquefaction occurs only locally within the sand.

6 REGRESSION ANALYSIS

The results of the parametric study were regressed to develop a design equation that could be used to derive estimates of liquefaction-induced settlements for typical residential buildings in the study area. Based on the trends identified between liquefaction-induced settlements and

various parameters from this study and following the Bray and Macedo (2017) approach, several functional forms were investigated to represent the total footing settlement due to liquefaction (i.e. including both co-seismic shear-induced and post-seismic reconsolidation settlements). The functional form that was selected based on the quality of fit to the available numerical results is given by the following equation:

$$\ln(s) = a_0 + a_1 \ln(Q) + a_2 B + a_3 H_{cr} + a_4 \ln\left[\tanh\left(H_{liq}\right)\right] + a_5 D_r + a_6 ln(D_{5-75}) + a_7 ln(Sa_{T=0.7s}) + \varepsilon \quad (1)$$

where s is the total (co-seismic plus post-seismic) liquefaction-induced settlement of the footing [cm], Q is the footing contact pressure (load) [kPa], B is the width of the footing [m], H_{cr} is the thickness of the non-liquefiable soil below the footing [m], H_{liq} is the thickness of the liquefiable soil layer [m], D_r is the relative density of the liquefiable soil [%], D_{5-75} is the significant duration of the motion at the free-field ground surface [sec], $S_{a,T=0.7s}$ is the 5%-damped spectral acceleration at 0.7sec period at ground surface [g], α_0=2.57, α_1=0.2, α_2=0.742, α_3=-0.454, α_4=1.924, α_5=-0.031, α_6=0.588, α_7=1.9, and σ=0.458.

When selecting ground motion intensity measures for the regression model, it was decided to use ground motion parameters that were readily available to the practitioners in in the study area. For this reason, the significant duration D_{5-75} at the ground surface and the 5%-damped spectral acceleration at 0.7sec period at the ground surface were selected for the regression model.

7 CONCLUSIONS

The paper presents an extensive study on the accumulation of liquefaction-induced settlements of existing residential houses in areas of moderate human-induced seismicity. Compared to previous relevant studies, the study addresses new challenges as it involves earthquakes of moderate intensity that do not cause complete soil liquefaction, and relatively narrow spread footings in lieu of rigid slab foundations. Analyses were performed with an advanced numerical methodology validated against observed behaviors of similar structures during the 2010–2011 Canterbury earthquakes in New Zealand. More than 500 parametric analyses were performed investigating the effect of critical soil, foundation, structure, and ground motion parameters. The results verify patterns observed in recent studies for slab foundations in high shaking areas and shed light to new mechanisms. For the low magnitude earthquakes considered in this study the total foundation settlements were found to be relatively limited. A simplified equation was also developed from regression of the numerical analyses results to derive estimates of liquefaction-induced settlements for residential buildings that was adopted in the latest update of the relevant building code for the area.

REFERENCES

BICL 2018. NAM Groningen Foundation Assessment- Geotechnical Assessment of 188 Williams St, Kaiapoi, New Zealand. Report, 14 February 2018.

Boulanger, R. W., and Idriss, I. M. 2014. CPT and SPT Based Liquefaction Triggering Procedures. Report No. UCD/CGM-14/01. Center for Geotechnical Modeling, UC Davis.

Boulanger, R. W., and Ziotopoulou, K. (2017). PM4Sand (version 3.1): A sand plasticity model for earthquake engineering applications. Report No. UCD/CGM-17/01, Center for Geotechnical Modeling, Department of Civil and Environmental Engineering, University of California, Davis, CA, March

Bray, J. D., and Macedo, J. 2017. 6th Ishihara lecture: Simplified procedure for estimating liquefaction-induced building settlement. *Soil Dynamics and Earthquake Engineering*, Elsevier, 102, 215–231.

Dashti, S., and Bray, J. D. 2013. Numerical Simulation of Building Response on Liquefiable Sand. *Journal of Geotechnical and Geoenvironmental Engineering*, 139(8), 1235–1249.

Giannakou,A.,Travasarou, T., Ugalde, J., Chacko, J.M., and Byrne, P. 2011. Calibration Methodology for Liquefaction Problems Considering Level and Sloping Ground Conditions, *5th International Conference on Earthquake Geotechnical Engineering*, Chile.

Green R.A., Bommer J.J., Stafford P.J., Maurer B.W.,Edwards B.,Kruiver P.P.,Rodriguez-Marek A., de Lange G., Oates S.J., Storck T., Omidi P., Bourne S.J., and van Elk J. 2018. Liquefaction Hazard Pilot Study for the Groningen Region of the Netherlands due to Induced Seismicity, prepared for NAM

Idriss, I.M. & Boulanger, R.W. 2008. Soil Liquefaction during Earthquake. *EERI Publication,Monograph MNO-12*, Earthquake Engineering Research Institute, Oakland.

Ishihara, K., and Yoshimine, M. 1992. Evaluation of settlements in sand deposits following liquefaction during earthquakes. *Soils and Foundations*, The Japanese Geotechnical Society, 32(1), 173–188.

Karamitros, D. K., Bouckovalas, G. D., and Chaloulos, Y. K. 2013. Insight into the Seismic Liquefaction Performance of Shallow Foundations. *J Geotechnical and Geoenvironmental Eng*, 139(4), 599–607.

Karimi, Z., Dashti, S., Bullock, Z., Porter, K., and Liel, A. 2018. Key predictors of structure settlement on liquefiable ground: a numerical parametric study. *SDEE*, Elsevier, 113, 286–308.

Naesgaard, E. and Byrne, P.M. (2007). "Flow liquefaction simulation using a combined effective stress - total stress model," 60th Canadian Geot Conf, Canadian Geotechnical Society, Ottawa, Ontario

Tasiopoulou, P., Giannakou, A., Drosos, V., Georgarakos, P., Chacko, J., de Wit, S., Zuideveld-Venema, N., 2018. Numerical evaluation of dynamic levee performance due to induced seismicity. *Bulletin of Earthquake Engineering*.

Taylor M.L., Cubrinovski M. and Bradley B.A. (2013). Cyclic strength testing of Christchurch sands with undisturbed samples. Proc. of NZSEE Conference, 26–28 April 2013, Wellington, New Zealand.

Wotherspoon LM, Orense RP, Bradley BA, Cox BR, Wood CM and Green RA (2013). Soil profile characterization of Christchurch strong motion stations. 13th NZSEE Conference

Ziotopoulou, K., and Boulanger, R. W. (2013) "Numerical Modeling Issues in Predicting Post-Liquefaction Reconsolidation Strains and Settlements." 10th Int Conf on Urban Eq Eng, Tokyo Institute of Technology, Tokyo, Japan.